Survey and Analysis of Underwater Acoustic Channels for Coherent Communication in the Medium-Frequency Band

Lee Freitag, Mark Johnson, Milica Stojanovic[†], Daniel Nagle[‡] and Josko Catipovic[‡]
Woods Hole Oceanographic Institution, Woods Hole, MA 02543
[†]Massachusetts Institute of Technology, Cambridge, MA 02139
[‡]Naval Undersea Warfare Center, Newport, RI 02841

Abstract— **A comprehensive set of acoustic communication data is analyzed using a complete receiver algorithm which includes a Doppler pre-processor, equalizer configuration algorithm and the decision feedback equalizer (DFE). The signal used for the tests is 1250 symbol per second QPSK (2500 bps) transmitted at a carrier of 2.25 kHz. Source-receiver ranges of up to 44 km were achieved at this data rate. The test environments include the New England Continental Shelf (less than 200 m), the shelf break (200-1200 m) and deep water (2500 m). In each environment the impulse response, the ambiguity function and the performance level of the receiver are presented. The link was very reliable to the maximum test range of 44 km on the shelf and to 20 km at the shelf break. In deep water the performance was good at less than 10 km and also at 35-44 km.**

I. Introduction

The performance of coherent acoustic communication systems is highly dependent upon channel characteristics including multipath, spatial and temporal coherence, Doppler effects and ambient noise. These effects change depending on local environmental conditions, the amount of movement of the source and receiver platforms and the beampatterns of the sonar transducers. While it is possible to accurately model many characteristics of the underwater sound channel, it is difficult to exactly reproduce the conditions under which an acoustic communication system will be used. Thus, comprehensive at-sea testing programs have been used to determine range, rate and reliability of specific implementations.

In 1996 a comprehensive acoustic communication test was carried out in order to establish the range and reliability level of phase-coherent modulation in the medium-frequency band. The test encompassed three major depth regimes: 100-200 m depth on the New England Continental Shelf, 200-1200 m deep-to-shallow propagation at the shelf transition, and south of the shelf in 2500 m water depth. The tests were performed with inter-platform relative motion of several meters per second, and source-receiver ranges which provide significant variability in signal-to-noise ratio (SNR).

The tests are motivated by the advantages of coherent signaling which include increased bandwidth efficiency over incoherent methods. However, creating a coherent underwater communications system that operates under a wide variety of conditions is very challenging. At issue is the configuration of the equalizer for different propagation conditions.

While recent advances in phase-coherent acoustic communications have demonstrated the potential for subsea telemetry, most published work has focussed on the development of the multi-channel decision-feedback equalizer [1], not the complete system in which it is used. In actual application, a coherent receiver requires Doppler processing, equalizer modifications to allow for very long-delay (sparse) multipath, and additional processing to ensure that the system is robust. The enhanced system uses settings which are established prior to runtime and then modified as conditions change. An equalizer configuration algorithm that automates the handling of these settings has been developed and its performance is demonstrated here. The impulse response estimate is used to create a multipath model for the equalizer and a training sequence is used to estimate the Doppler shift. The configuration algorithm allows reliable communication successfully and automatically under conditions of rapid change.

Receiver results are only a part of what is needed to understand how the acoustic channel impacts system performance. The data must also be analyzed in terms of delay and Doppler spread to allow system performance to be understood in a heuristic sense. These effects heavily influence the acoustic communication receiver and thus these measures accompany the presentation of receiver performance.

Phase-coherent acoustic communication test results in the frequency range of 1 to 3 kHz have been reported by several researchers. The first long-range experiments were carried out in the Pacific in 1991 and achieved 1000 bits per second at 200 km (3 convergence zones) using a carrier frequency of 1 kHz [1]. Similar experiments were carried out on the New England continental shelf in 1992 and achieved up to 2000 bps at 83 km [1]. These ranges and rates are the highest reported in the literature (see [2] for a recent comprehensive survey). Additional tests in this frequency regime include those performed in the Mediterranean in 1994 at 50 km using 212 bps BPSK at

This work was supported by the Office of Naval Research. Email contact: lfreitag@whoi.edu.

0-7803-6551-8/00/$10.00 ©2000 IEEE

a carrier of 1.7 kHz [3] [4]. In both cases the reported results are indicative of receiver performance in isolated cases. In addition, the source-receiver velocity is near zero for all of these experiments.

The contributions of this paper include a brief description of the multi-channel receiver, as well as receiver performance results in multiple propagation regimes with significant variation in range, SNR, delay spread and Doppler shift. The paper is organized as follows. Section II is a review of the receiver and a summary of important issues. Section III describes the metrics used to evaluate and categorize the experimental data. Section IV describes the test conditions and the results.

II. The Receiver

In a typical coherent acoustic communication system, data is transmitted in short packets beginning with an acquisition signal and a short delay, followed by a block of training symbols, and then the data symbols. The receiver takes advantage of information about the channel available from the acquisition signal and training sequence.

The receiver has as its kernel, the sparse DFE [5] which consists of a multi-channel fractionally-spaced combiner together with a sparse decision feedback section [5]. Both the multi-channel combiner and the feedback section are implemented as a bank of jointly-adapted FIR filters. A phase-locked loop (PLL) is also embedded in the equalizer as part of the Doppler mitigation strategy. The overall receiver structure includes a pre-processor (Fig. 1) with Doppler estimator and sample-rate correction [6] and an equalizer tap-placement algorithm. This is followed by the decision feedback equalizer and subsequently by error-correction decoding.

A. Doppler Pre-Processor

In the results presented here Doppler compensation is implemented as a batch process prior to equalization. First the frequency shift is estimated from the training data using the ambiguity function. For efficiency, the ambiguity function is computed across a coarse range of Doppler shifts and only at the time lags corresponding to the main arrivals. Doppler compensation is accomplished by first adjusting the carrier phase shift and then interpolating the signal to correct the sample rate. The Doppler pre-processor is described in detail in [6].

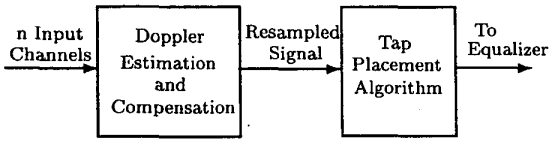

Fig. 1. Receiver pre-processor.

B. Tap Placement

The variation in the acoustic channel can be large when source or receiver are in motion. As a result the multipath structure changes both on small scales (individual ray amplitude variation) and large scales (gross changes in the acoustic field). The tap-placement algorithm is used on each packet to determine the number of coefficients in the feedforward and feedback filters. This is done by simple thresholding of the impulse response and identifying the lags where significant multipath is present. In addition to the filter size estimates, the algorithm is used to determine the position of the reference tap of the equalizer, i.e. the temporal position of the start of the feedback filter. While the thresholding technique provides good first-order estimates of filter sizes and positions for many cases, performance drops at low SNR and it does not take into account the beamforming capabilities of the multi-channel equalizer. A tap placement algorithm which offers more optimization (though at a price in complexity) is presented in [7].

C. Equalizer

The multi-channel DFE with 2nd order phase-locked loop operates on the Doppler compensated data using the filter configurations determined during the tap-placement step. The delay spread of the channel sets the feedforward and feedback filter widths which then determines the tracking ability of the equalizer and its computational complexity.

Tracking and computational complexity are also influenced by the choice of update algorithm. Recursive least-squares (RLS) and several varieties of the least-mean-square (LMS) are among the most commonly used update algorithms. The adaptive LMS adjusts the step size μ to provide a balance between tracking rate and excess mean-square error (MSE) which occurs when the tracking rate is higher than necessary [8]. The adaptive-μ LMS offers a good compromise between complexity and performance and is used for the analysis in this paper. A detailed description of the equalizer and direct comparison between the LMS and RLS for adaptive equalization in the underwater channel may be found in [9].

By far the dominant factor in the performance of coherent receivers in the underwater channel is the number of array channels used by the equalizer [9]. It is not uncommon for the average MSE for a single channel to be -2 or -3 dB and unsuitable for reliable DFE operation with BPSK modulation. However, using 8-16 channels may provide -15 to -20 dB MSE, sufficient to support 8-PSK or 16-QAM signaling.

Additional features of the receiver include:

Reduced Filter Updating. In many acoustic environments the multipath structure varies rather slowly with time. In such cases, the adaptive filters need only be updated

during training and then when performance deteriorates due to accumulated environmental change. One method for minimizing computational complexity is to update the filters only when a recursive measure of the MSE exceeds a pre-set threshold. The time constant of this estimator determines how fast the equalizer will respond to a change in the environment and should be chosen so as to prevent updating as a result of transients. A first-order recursive MSE estimator with a pole position of 0.95 offers a good compromise between smoothing and tracking capability in the channels analyzed here.

Error Limiting. The effect of impulsive biologic or man-made noise in the received signal can be partially mitigated by soft-limiting the error signal before using it to update the equalizer parameters. This technique, borrowed from outlier removal techniques in least-squares estimation, effectively reduces the size of the divergent innovation made by the equalizer in response to an impulsive input. Soft-limiting the error e with the limiting factor g using the hyperbolic tangent function is done by

$$e' = e\frac{\tanh(g|e|)}{g|e|}$$

where g is set to 1 in impulsive environments and near 0 in AWGN. A slight penalty in training and tracking occurs when this function is used, but it helps prevent catastrophic divergence of the DFE in conditions where shrimp, sperm whales or long-baseline tracking pings are in or near the communications band.

III. Data Analysis Methods

The metrics used for the detailed analysis include a single measure of the impulse response estimated by match filtering the channel probe at the start of each packet, and the ambiguity function computed over approximately 1000 symbols (0.8 seconds).

The Doppler spread of the complex baseband signal $\mathbf{y} = [y_k, \ldots, y_{k+n-1}]$ sampled at twice the maximum frequency $1/T$ is estimated using the known transmitted symbols $\mathbf{d}$ via the ambiguity function. To do so the transmitted replica is time compressed and phase-shifted at each candidate Doppler factor ν so that $\mathbf{y}'(\nu) = \mathcal{S}(\nu, \mathbf{y}\exp(-j2\pi\nu\mathbf{t}))$ where $\mathcal{S}(\nu, \cdot)$ is a suitable interpolation function and $\mathbf{t} = 0, 1, \ldots, n-1$. The ambiguity function is

$$A(\nu) = \mathcal{F}^{-1}[Y(\nu)D^*(\nu)]$$

where $Y = \mathcal{F}(\mathbf{y})$ and $D = \mathcal{F}(\mathbf{d})$ are the Fourier transforms of $\mathbf{y}$ and $\mathbf{d}$ respectively. While the transmitted data are random and do not have periodic autocorrelation with low side-lobes [10], the multi-Doppler matched filtering (MDMF) processor provides a reasonable estimate of the channel ambiguity function.

IV. Results

During the tests described below 1250 symbol per second QPSK data (2500 bit per second) signals were transmitted in 6 s long packets at 15 s intervals. Each packet contained 1568 bytes of raw data or 1 kB after error-correction coding. The signals were transmitted at a carrier frequency of 2.25 kHz and occupied a 3 dB bandwidth of 1250 Hz. A two-element array was towed by the source vessel. In shallow water the receiver was a 16-channel vertical array with 1 m element spacing suspended at 70 m. In deep water a 16-channel array with 6 m element spacing was placed at 700 m. In both cases the receive vessel drifted freely.

A. Continental Shelf Propagation

The first experiment was conducted on the Continental Shelf in water depths of 100-200 m and ranges of 6 to 44 km and speeds of 0-3 m/sec. Three sound speed profiles along the track of the source vessel are shown in Fig. 2. The ray paths for the first 15 km of propagation are shown in Fig. 3. The drift track of the receiver and the route taken by the transmitter vessel are shown in Fig. 4.

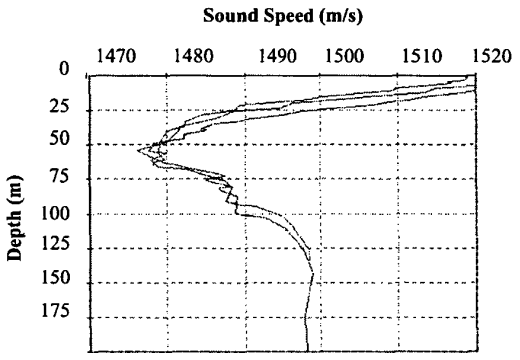

Fig. 2. Sound speed in shallow water.

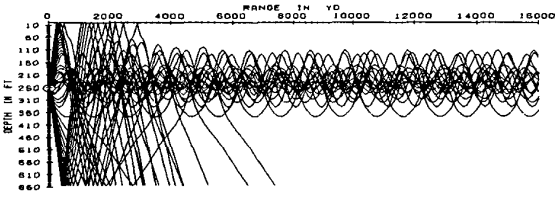

Fig. 3. Ray paths in shallow water.

The impulse response and angle of arrival pattern at 6 km is shown in Fig. 5. An initial group of arrivals spanning 20 ms is followed by sparse arrivals with a total duration of 150 ms. The angle of arrival distribution shows the lower-angle rays arriving first, followed by the smaller-amplitude, higher-angle rays. The amplitude of the later rays slowly decrease as range increases, and as they dis-

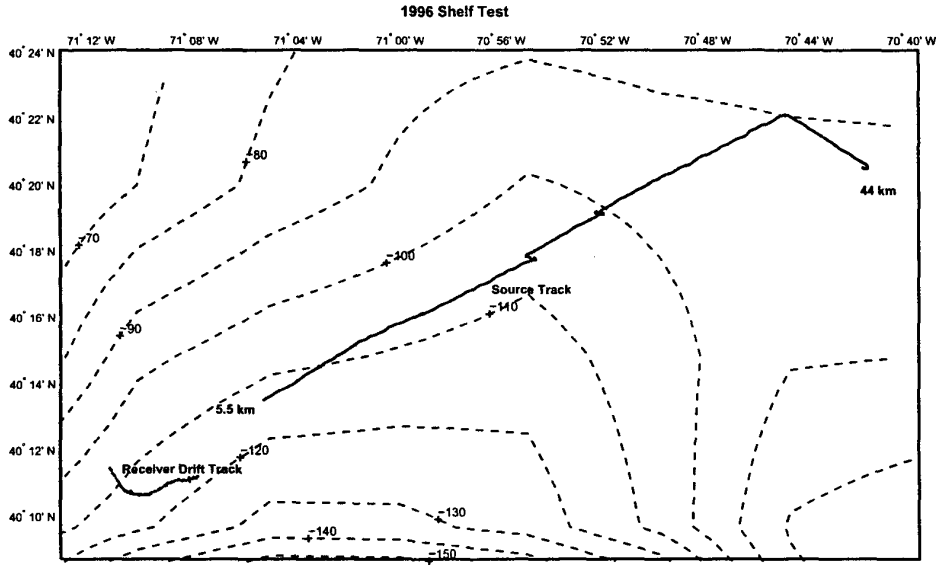

Fig. 4. Source and receiver locations for the shallow-water test. The packet success rate exceeded 98%.

appear the first 40-50 ms of the channel response become increasingly dense. The ambiguity function at close range is shown in Fig. 6. It shows an overall shift of approximately 3 Hz, and spreading of approximately 1 Hz.

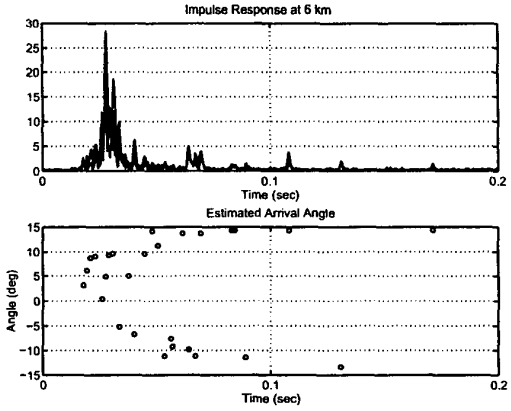

Fig. 5. Impulse response and angle of arrival at 6 km.

The impulse response and angle of arrival pattern at 44 km is shown in Fig. 7. A dense response with many arrivals of similar amplitude are distributed over 70 ms. The angular spread is less than at close-range, approximately ±10°. In Fig. 8 the ambiguity function for the

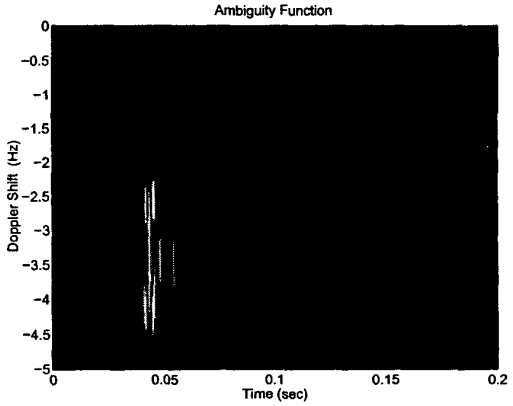

Fig. 6. Ambiguity function at 6 km range in shallow water.

44 km case is shown. Here the velocity is essentially zero (both ships were drifting) and the overall Doppler shift is very small. All of the arrivals at this range have nearly the same Doppler spread, which is no greater than that observed at 6 km.

Results from the shallow-water test using the receiver described in Section II are shown in Fig. 9. The test spanned seven hours and included both moving and stationary sections. The Doppler shift is estimated automat-

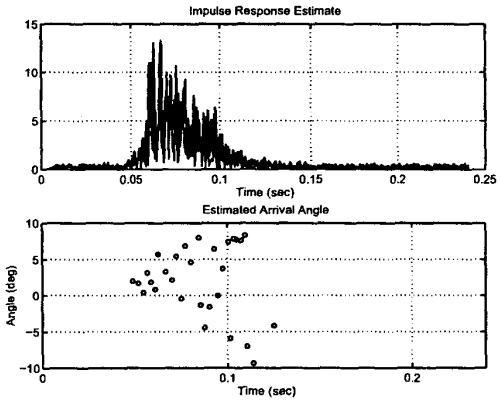

Fig. 7. Impulse response and angle of arrival at 44 km.

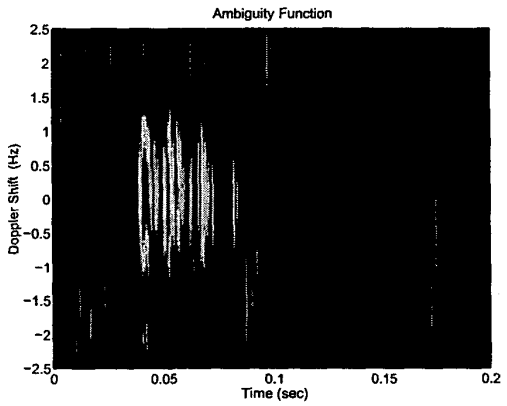

Fig. 8. Ambiguity function at 44 km range in shallow water.

ically, as are the number of equalizer parameters and their placement. The average MSE is plotted to indicate the performance level at the output of the equalizer. While only -8 dB is necessary for reliable decision-directed operation using QPSK modulation, the average MSE is usually much lower than that, and often less than -15 dB. Thus this link could support trellis-coded 8-PSK which would allow a 50% increase in throughput.

The overall reliability is very good–over 98% of the packets are received error-free. Several factors directly contribute to this excellent success rate. One, ducting minimizes surface and bottom interaction which reduces boundary loss and scatter; two, the SNR is very high; and three, despite the overall Doppler *shift* the Doppler *spread* is low. There is a small difference in performance between the stationary and the moving sections of the test, particularly at close range. At long range (42 km), the average MSE increases slightly as the source vessel changes course and the propagation conditions change. At the very end of the test when the velocity goes to zero the average MSE again improves.

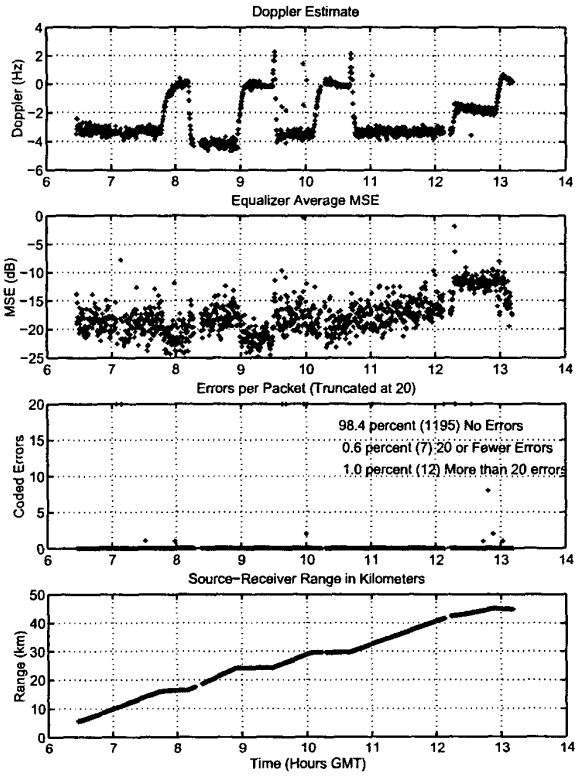

Fig. 9. Results summary from shallow water testing.

B. Shelf-break Propagation

At the edge of the New England Continental Shelf the bottom slopes from 150 m to 1500 m in less than 50 km (Fig. 11). The multipath in this environment is very complex, both at close and long ranges. The modeled ray paths and transmission loss are shown in Fig. 10. Here again, ducted conditions exist which provide for long-range propagation. At close range some rays interact with both bottom and surface, which creates considerable complexity. At 7 km the arrival structure is very long (Fig. 12) and is a combination of specular and diffracted arrivals. The total length is 200 ms and several hundred fractionally-spaced feedforward taps are necessary to span it. Despite this complexity, the acoustic channel provides reliable communication due to the high SNR and stability of the primary paths. At 37 km (Fig. 13) the time spread is 100 ms and the arrival structure appears incoherent from hydrophone to hydrophone. The early rays are low amplitude which makes it difficult to determine where the packet begins. Long feed-forward filters are also used here in order to capture and combine as much of the

energy as possible. The ambiguity function at this range (not shown) does not reveal significant Doppler spread, though the peaks are shifted due to the relative motion of the source and receiver.

The results of processing the entire four-hour segment spanning 7 to 37 km is shown in Fig. 14. At close range (7 to 13 km) the channel has high complexity due to the surface and bottom interaction. However, from 13-20 km the reliability is very good, so that on average from 7-20 the success rate is over 90% In the range from 20-37 km the performance slowly degrades. The SNR is significantly lower than in shallow water, and the multipath is much longer as well. The average success rate for this segment is still over 60%, which is quite good considering the 1250 symbol per second rate and the difficulty of the acoustic channel.

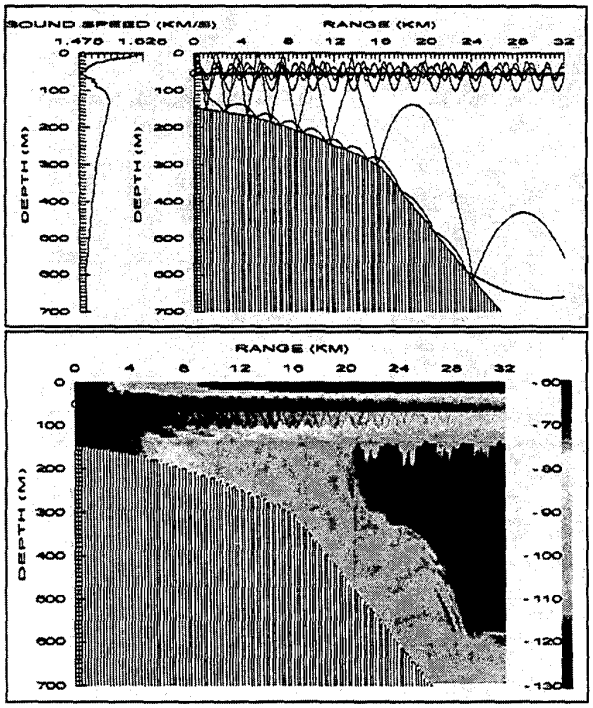

Fig. 10. Paths and transmission loss at the shelf break.

C. Deep-Water, Close-Range Propagation

The deep-water tests were conducted near 39 deg N, 71 W in water 2500 m deep. The performance at very close range when the direct path is the dominant arrival is good. However, as range increases past 10 km, the energy in the direct path becomes only a fraction of the total energy seen at the receiver. As shown in Fig. 15, the multipath includes direct, bottom and surface-bottom paths and the delay spread is almost one second. The very long delay spread presents significant difficulty for

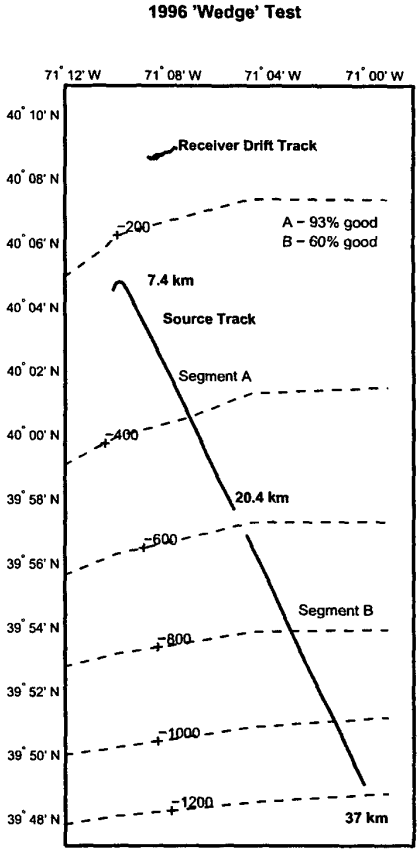

Fig. 11. Source and receiver locations for the deep-to-shallow test.

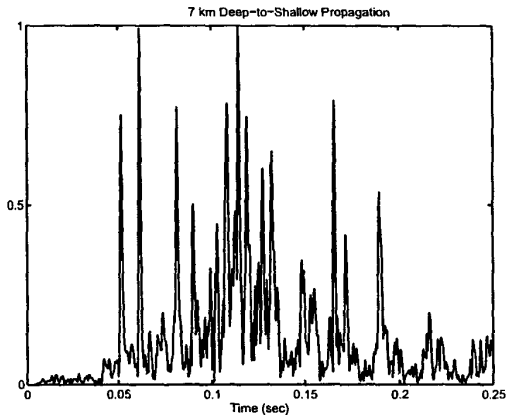

Fig. 12. Impulse response at the shelf break at 7 km.

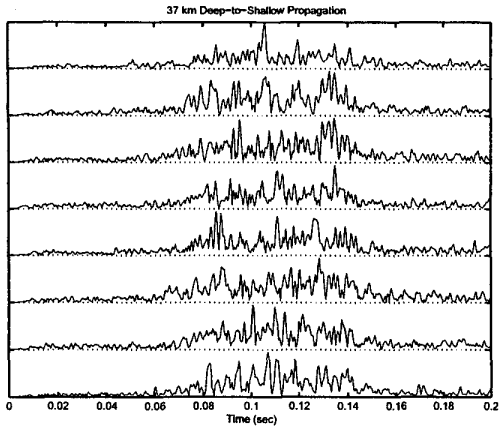

Fig. 13. Array impulse response at 37 km.

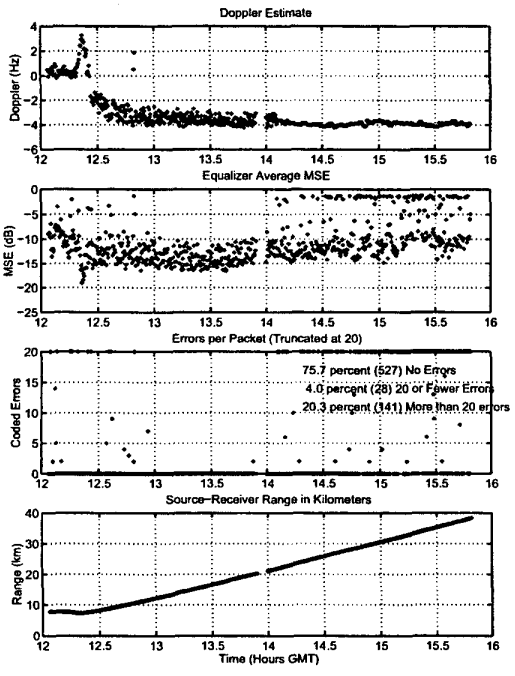

Fig. 14. Results summary from shelf-break testing.

coherent (or incoherent) acoustic communication due to the large ratio of scattered-to-direct energy and the long delay between arrivals.

However, the system can operate in these environmental conditions when the equalizer can combine n channels with short feedforward filters such that the residual, uncompensated ISI from the scattered rays is a fraction of that recovered from the initial group. An example of this case is shown in Fig. 16 where the SNR is slightly greater than in Fig. 15 and the surface and bottom reflected ray groups span less than 20 ms each. When the receiver focuses on the main arrival, which itself shows 10 ms spread, the other groups (which arrive at significantly different angles) have lower combined energy at the output of the equalizer than the direct path. Thus, despite the 0.8 s delay spread, the receiver operates successfully on this channel using the vertical array.

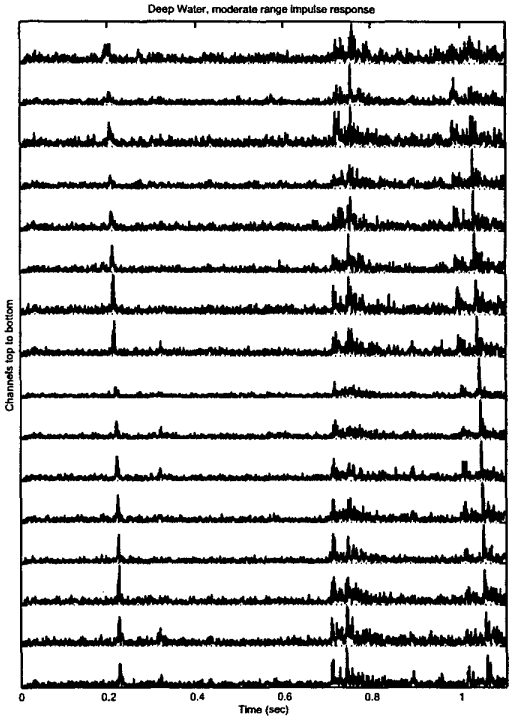

Fig. 15. Impulse response at 17 km in deep water.

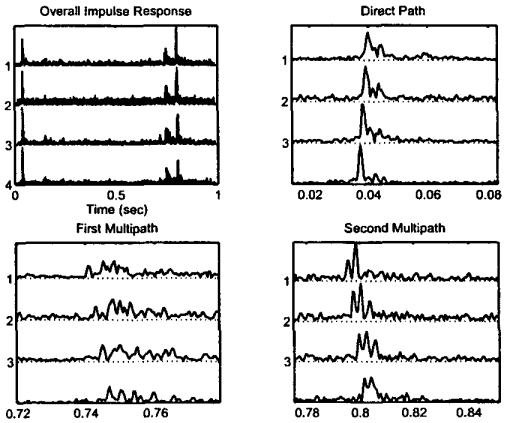

Fig. 16. Impulse response at 11 km in deep water.

D. Deep-Water, Long-Range Propagation

During the deep-water test the propagation conditions provided a partial convergence zone at 35-44 km. As shown in Fig. 17, two rays are present with a slight difference in Doppler shift and spread. The long range channel is very simple and it provides excellent reliability throughout the region where the rays refracting toward the surface intercept the receiver. Only four hydrophones are required to achieve full-rate QPSK, and processing the entire 16 element array provides MSE adequate for 8-PSK.

While the acoustic propagation conditions in deep-water were very good, the background noise level was high due to sperm whales in the area. The overall reliability of the link was maintained through use of the error-limiting function and error-correction coding.

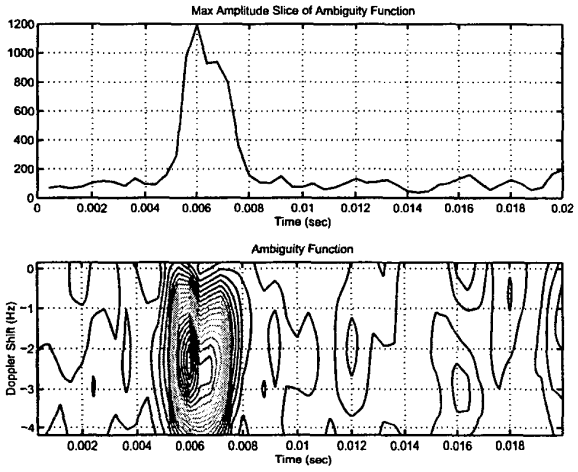

Fig. 17. Impulse response and ambiguity function in deep water.

V. Conclusion

A complete acoustic communications receiver which has the capability of autonomously setting many of its operational parameters using information available from the signal has been developed. Using the DFE as a kernel, the new receiver estimates and corrects Doppler shift on the received signal and chooses appropriate sizes for both the feedforward and feedback filters in the equalizer. Moreover, the computational requirements change with the complexity of the environment. Very low computational rates are obtained when the channel is stable or has a sparse impulse response.

Results demonstrate that the receiver provides 60-98% packet success rate in a time-varying acoustic environment. In shallow water the propagation conditions during the test period provided very good performance and continuous connectivity. At the shelf break the complex bathymetry creates multipath with very long duration at close range, though the stability of the many boundary-interacting rays is good, allowing most data to be decoded successfully at 1250 sps. As range increases, the conditions become ducted and the multipath includes many rays of similar amplitude with little apparent correlation from channel to channel. While the impulse response appears very difficult, a large fraction of the data from 20-37 km in the deep-to-shallow regime decodes correctly.

In deep water the performance of the system is also highly dependent on the propagation conditions. At close range the bottom scatter limits performance to geometries where the direct path contains sufficient energy to counteract the reflected rays with long delay. Under these conditions the vertical array is important because the multichannel receiver can focus upon the initial arrival and effectively null some of the out-of-plane scatter. Deep-water propagation at long range (35-44 km in this test) provides very good performance due to the simplicity of the received signal. Array processing provides significant gain and the throughput of the link scales with the number of available hydrophones.

Acknowledgements

The authors would like to thank J. Cooper and C. Eck of WHOI and the R/V Sea Diver and R/V Seward Johnson for excellent field support. Propagation modeling software and support was provided by R. Keenan of SAIC.

References

[1] M. Stojanovic, J. Catipovic and J. Proakis, "Adaptive multichannel combining and equalization for underwater acoustic communications", *J. Acoustic Soc. Am.*, **94** (3), Pt. 1, pp. 1621-1631, Sept. 1993.

[2] D. Kilfoyle and A. Baggeroer, "The state of the art in underwater acoustic telemetry," *IEEE J. Oceanic Eng.*, Vol. 25, pp. 4-27, Jan. 2000.

[3] V. Cappellano, G. Loubet and G. Jourdain, "Adaptive multichannel equalizer for underwater communication," *Proc. Oceans'96,* Ft. Lauderdale, pp. 994-999.

[4] D. Thompson, et. al., "Performance of coherent PSK receivers using adaptive combining, beamforming and equalisation in 50 km underwater acoustic channels," *Proc. Oceans'96,* Ft. Lauderdale, pp. 845-850.

[5] M. Johnson, D. Brady, M. Grund, "Reducing the computational requirements of adaptive equalization in underwater acoustic communications", *Proc. Oceans '95,* San Diego, Sept. 1995.

[6] M. Johnson, L. Freitag and M. Stojanovic, "Improved Doppler Tracking and Correction for Underwater Acoustic Communication," in *Proc. ICASSP'97,* vol 1, pp. 575-578, Munich, Germany, April, 1997.

[7] M. Lopez, A. Singer, S. Whitney and G. Edelson, "A DFE coefficient placement algorithm for underwater digital acoustic communications", *Proc. Oceans '99,* pp. 996-1001, Seattle, Sept. 1999.

[8] S. Haykin, *Adaptive Filter Theory,* 3rd Edition, New Jersey: Prentice Hall, 1996.

[9] L. Freitag, M. Johnson and M. Stojanovic, "Efficient equalizer update algorithms for acoustic communication channels of varying complexity," *Proc. Oceans '97,* pp. 580-585, Oct. 1997.

[10] D. Mauuary, G. Jourdain and T. Terre, "Fast ambiguity processing in SOFAR propagation involving periodic signals and M-sequences", *IEEE Proc. Sig. Proc.*, vol. 46, No. 8, Aug. 1998.